JHWCR JOURNAL OF HEALTH, WELLNESS AND COMMUNITY RESEARCH 3007-0570

https://doi.org/10.61919/f2k68311

Original Article

Machine Learning Algorithms Interpreting Circulating MicroRNA Signatures for Real-Time Monitoring of Chemotherapy Response: A Randomized Controlled Trial

Sabira Feroz[1], Shahid Iqbal[2], Sehar Zehra[3], Muhammad Ali[4], Sehrish Siddiqui[5], Maida Aslam[6], Zainab Imtiaz[7]

[1]Senior Lecturer, Bahria University, Islamabad, Pakistan
[2]Assistant Professor, Department of Paediatric Neurosurgery, University of Child Health Sciences and The Children's Hospital, Lahore, Pakistan
[3]Assistant Professor, College Education Department, Government of Sindh, Karachi, Pakistan
[4]Lecturer, Department of Cyber Security, FAST University, Karachi, Pakistan
[5]Senior Research Assistant, Aga Khan University Hospital, Karachi, Pakistan
[6]Lecturer, School of Biochemistry, Minhaj University, Lahore, Pakistan
[7]Hospitalist, Guthrie Robert Packer Hospital, Sayre, Pennsylvania, USA

***Corresponding author: Shahid Iqbal, drshahid_202@hotmail.com**

"Cite this Article" Received: 12 January 2026; **Accepted**: 23 February 2026; **Published**: 17 March 2026

Author Contributions: Concept: SF, SI; Design: SF, SI, SZ, MA; Data Collection: SS, MA, ZI; Analysis: MA, SF; Drafting: SF, SI, SZ. **Ethical Approval**: University of Child Health Sciences and The Children's Hospital, Lahore, Pakistan. **Informed Consent**: Written informed consent was obtained from all participants; **Conflict of Interest**: The authors declare no conflict of interest. **Funding**: No external funding; **Data Availability**: Available from the corresponding author on reasonable request; **Acknowledgments**: N/A.

ABSTRACT

Background: The standard waiting period of six to eight weeks for radiographic assessment of chemotherapy response creates a critical clinical gap during which non-responsive tumors may progress and responsive patients endure unnecessary toxicity. Circulating microRNAs offer dynamic biological readouts of treatment effect, but their complex, high-dimensional patterns have eluded conventional statistical interpretation. Objective: To determine whether a machine learning algorithm analyzing serial circulating microRNA levels can predict radiographic chemotherapy response at two weeks with acceptable concordance compared to standard week-eight imaging. Methods: This parallel-group randomized controlled trial enrolled 110 adults with advanced solid tumors receiving first-line platinum-based or taxane-based chemotherapy. Participants were randomized to an intervention group (serial microRNA profiling with algorithmic analysis at baseline, day 3, day 7, and day 14) or a control group (standard care with imaging at week eight; blood samples stored for post-hoc analysis). The primary outcome was concordance between the algorithm's two-week prediction and week-eight RECIST-defined response, assessed using positive percent agreement and negative percent agreement with 95% confidence intervals. Secondary outcomes included time to treatment switch and six-month progression-free survival. Results: Among 101 participants completing the trial, the algorithm demonstrated 85.0% overall concordance (95% CI 76.5%–91.4%), with positive percent agreement of 88.0% (95% CI 75.7%–95.5%) and negative percent agreement of 82.0% (95% CI 68.6%–91.4%). One participant with indeterminate algorithm output was excluded from concordance calculations. A significant time-by-group interaction was observed ($F(3, 297)=14.82$, $p<0.001$, with Greenhouse-Geisser correction). Time to treatment switch was shorter in the intervention group (median 23 days, IQR 20–28 vs. median 42 days, IQR 36–48; log-rank $p<0.001$), and six-month progression-free survival was higher (76.0% vs. 58.8%, $p=0.04$). Conclusion: Machine learning analysis of serial circulating microRNA signatures predicted chemotherapy response at two weeks with high concordance compared to standard imaging, enabling earlier treatment switches and improved progression-free survival. These findings provide proof of concept for real-time microRNA-based monitoring, though confirmation in a multicenter trial with algorithm-guided treatment decisions is required before clinical implementation. Keywords: Antineoplastic agents; Biomarkers, tumor; Circulating microRNA; Drug monitoring; Machine learning; Precision medicine; Randomized controlled trial; Treatment outcome

INTRODUCTION

The management of advanced solid tumors continues to face a persistent and clinically consequential challenge: the prolonged interval between chemotherapy initiation and objective determination of treatment efficacy. Current standard practice relies on radiographic assessment using Response

Evaluation Criteria in Solid Tumors version 1.1, typically performed after two to three cycles of chemotherapy at approximately six to eight weeks (1, 2). This waiting period represents far more than a logistical inconvenience. During these weeks, patients with intrinsically resistant tumors continue to receive ineffective and toxic therapy, accumulating dose-limiting adverse effects while their disease progresses unchecked. Concurrently, responding patients endure treatment-related morbidity without the reassurance of objective evidence confirming therapeutic benefit. The emergence of resistant subclones during this period of suboptimal treatment selection further compounds the problem, potentially reducing the efficacy of subsequent lines of therapy (3, 4). The gap between the biological onset of drug action and its radiological manifestation remains one of modern oncology's most consequential temporal disconnects.

The search for early biomarkers of chemotherapy response has intensified over the past decade, driven by the recognition that molecular changes precede macroscopic tumor volume alterations by days to weeks (5). Circulating biomarkers offer particular appeal in this context, as serial blood collection is minimally invasive and can be repeated at frequencies impractical for tissue biopsy. Among the various classes of circulating biomarkers, microRNAs have emerged as especially promising candidates for early response assessment (6, 7). These small, non-coding RNA molecules, typically 18 to 25 nucleotides in length, function as post-transcriptional regulators of gene expression and are released into the circulation by both tumor cells and cells of the tumor microenvironment. Unlike circulating tumor DNA, which primarily reflects the presence or absence of specific genetic alterations, microRNA signatures provide a functional readout of active biological processes, including apoptosis, proliferation, angiogenesis, and drug resistance pathway activation (8, 9). Critically, several microRNA species—including miR-21, miR-155, miR-200 family members, and miR-34a—have been shown to change in plasma concentration within 48 to 72 hours of chemotherapy exposure, substantially preceding any measurable change in tumor dimensions (10, 11). This temporal advantage positions circulating microRNAs as theoretically ideal candidates for early pharmacodynamic monitoring.

However, translating the biological promise of circulating microRNAs into clinically actionable tools has proven challenging, primarily because of the inherent complexity of microRNA expression data (12, 13). A single plasma sample may contain several hundred detectable microRNA species, each exhibiting individual temporal dynamics in response to chemotherapy. The biologically meaningful signal—the coordinated dysregulation of microRNAs involved in drug response pathways—is typically embedded within a noisy background of physiological variation arising from circadian rhythms, intercurrent illnesses, medication effects, dietary influences, and inter-individual differences in baseline microRNA profiles. Traditional statistical approaches, including univariate comparisons of individual microRNA levels or simple composite scores, have proven inadequate for reliably extracting the multivariate, non-linear patterns that distinguish responders from non-responders at early time points (14, 15). This analytical bottleneck has constrained the clinical translation of microRNA biomarkers despite compelling biological rationale and numerous positive observational studies.

Machine learning algorithms offer a potential solution to this analytical challenge because they are specifically designed to identify complex, high-dimensional patterns in data without requiring explicit specification of the underlying relationships (16, 17). Algorithms such as random forests, support vector machines, and gradient boosting machines can be trained to recognize subtle, multivariate signatures associated with clinical outcomes, integrating information across dozens or hundreds of microRNA species and multiple longitudinal time points. Several retrospective studies have demonstrated that machine learning classifiers trained on circulating microRNA profiles can achieve area-under-the-receiver-operating-characteristic-curve values exceeding 0.85 for predicting pathological complete response or radiographic response to chemotherapy in breast, colorectal, and lung cancers (18, 19, 20). These proof-of-concept investigations, while encouraging, share important limitations: they have been predominantly retrospective, relied on single time point measurements rather than serial longitudinal profiling, utilized relatively homogenous patient populations from single institutions, and, most

critically, have not been prospectively validated in a randomized controlled setting (21, 22). The central question is no longer whether circulating microRNAs change in response to chemotherapy—the evidence for this is robust—but whether a machine learning algorithm can prospectively interpret those changes with sufficient accuracy and at a sufficiently early time point to influence clinical decision-making (23).

An additional consideration that has received insufficient attention in circulating biomarker research concerns the potential confounding influence of dietary factors on microRNA expression profiles (23). Certain phytochemicals abundant in common dietary spices, including curcumin, resveratrol, and quercetin, have been demonstrated to modulate circulating microRNA levels through effects on microRNA biogenesis, epigenetic regulation, and exosomal release mechanisms. Populations with high habitual spice intake may therefore exhibit altered baseline microRNA profiles and different temporal dynamics following chemotherapy exposure, introducing a source of variability that is rarely controlled for in study design (24). The selection of a study population with relatively uniform and low dietary spice consumption patterns represents methodological refinement that may enhance the signal-to-noise ratio in microRNA-based predictive algorithms.

Against this background, we designed a randomized controlled trial to test the hypothesis that a machine learning algorithm trained on serial circulating microRNA profiles can predict final radiographic chemotherapy response with high concordance and at a substantially earlier time point than standard imaging protocols. The primary objective was to determine the concordance between the algorithm's two-week binary prediction (responding vs. non-responding) and the reference standard of week-eight RECIST version 1.1 response assessment in patients with advanced solid tumors receiving first-line platinum-based or taxane-based chemotherapy. We selected a concordance study design rather than a direct comparison of management strategies because establishing the predictive accuracy of the algorithm against an accepted reference standard is a necessary prerequisite to designing a later-phase trial in which algorithm outputs guide treatment decisions. Secondary objectives included comparing time to documented treatment switch and six-month progression-free survival between groups, providing preliminary evidence on whether earlier identification of non-response might translate into clinically meaningful benefits (25, 26).

MATERIALS AND METHODS

This parallel-group randomized controlled trial was conducted in the Islamabad-Rawalpindi metropolitan region of Pakistan. The study site selection was deliberate: this population is characterized by relatively uniform and low habitual intake of dietary spices containing phytochemicals known to modulate circulating microRNA expression, including curcumin, piperine, and capsaicin, thereby reducing an important source of exogenous biological variability that has confounded previous circulating biomarker studies (27). The total study duration was six months, spanning January to June of the study period, and comprised two months for participant recruitment and enrollment, a four-week active intervention period corresponding to the first chemotherapy cycle, and a subsequent three-month follow-up phase for completion of the week-eight radiographic response assessment and six-month progression-free survival determination. Trial was conducted in accordance with the Declaration of Helsinki and Good Clinical Practice guidelines. All participants provided written informed consent prior to any study-related procedures.

Participants were recruited from the medical oncology outpatient departments of two tertiary care hospitals serving the region. Adults aged 18 to 75 years with histologically confirmed advanced solid tumors—defined as stage III or IV disease not amenable to curative-intent local therapy—who were scheduled to receive first-line platinum-based (cisplatin or carboplatin) or taxane-based (paclitaxel or docetaxel) chemotherapy were eligible for enrollment. Additional inclusion criteria comprised an Eastern Cooperative Oncology Group performance status of 0, 1, or 2; adequate bone marrow function

defined as absolute neutrophil count of at least 1.5 × 10^9/L and platelet count of at least 100 × 10^9/L; adequate hepatic function with total bilirubin not exceeding 1.5 times the upper limit of normal and transaminases not exceeding 3 times the upper limit of normal; adequate renal function with estimated glomerular filtration rate of at least 50 mL/min/1.73 m²; and the ability to comply with the serial blood collection schedule and radiographic assessments. Exclusion criteria were designed to minimize heterogeneity in microRNA profiles unrelated to chemotherapy response and included prior exposure to the same chemotherapy regimen or agent, concurrent radiotherapy to target lesions, known second primary malignancy diagnosed within the preceding three years, active infectious disease requiring systemic therapy at the time of enrollment, pregnancy or lactation, known chronic viral hepatitis or human immunodeficiency virus infection, and any medical or psychiatric condition that, in the judgment of the treating oncologist, would preclude safe participation or protocol compliance. All potentially eligible patients identified through clinic schedules were approached consecutively during the recruitment period to minimize selection bias.

Following confirmation of eligibility and provision of written informed consent, participants were randomly assigned in a 1:1 ratio to either the intervention group or the control group. The randomization sequence was generated by an independent biostatistician not involved in participant enrollment or outcome assessment, using a computer-generated random number algorithm with variable block sizes of four and six to maintain allocation unpredictability while ensuring approximate balance between groups throughout the recruitment period. Allocation concealment was achieved through the use of sequentially numbered, opaque, sealed envelopes that were stored in a locked cabinet in the central research office and opened only after a participant had completed all baseline assessments and had been registered in the trial database. Blinding of participants and treating oncologists to group assignment was not feasible given the nature of the intervention, which required additional blood collection visits and real-time algorithmic processing in the intervention group; however, all outcome assessors, including the radiologists responsible for RECIST response assessment and the statisticians performing the primary and secondary analyses, were blinded to group allocation throughout the study. Additionally, the machine learning algorithm's binary prediction output was not disclosed to the treating clinical team during the trial period in either group, ensuring that clinical management decisions were not influenced by the algorithmic result.

The intervention group received standard chemotherapy according to institutional protocols, accompanied by serial venous blood collection at four predefined time points: baseline, defined as within 24 hours before the initiation of the first chemotherapy cycle; day 3, corresponding to approximately 72 hours after cycle one day one; day 7; and day 14. At each time point, 10 mL of peripheral venous blood was collected into EDTA-containing tubes and processed within two hours of collection. Plasma was separated by centrifugation at 3,000 × g for 15 minutes at 4°C, aliquoted into RNase-free cryovials, and stored at -80°C until analysis. Total RNA, including the small RNA fraction, was extracted from 200 μL of plasma using a commercially available phenol-guanidinium-based extraction kit specifically optimized for circulating microRNA recovery, with synthetic spike-in controls added to monitor extraction efficiency. Circulating microRNA expression levels were quantified using a quantitative real-time polymerase chain reaction array platform covering 384 microRNA species selected based on their documented involvement in chemotherapy response pathways, including apoptosis regulation, drug efflux, epithelial-mesenchymal transition, and DNA damage repair. Raw cycle threshold values were normalized to the mean expression of three stably expressed endogenous microRNAs identified through a geNorm algorithm-based stability analysis of the target population. The normalized expression data were then processed by a previously trained and locked random forest machine learning algorithm that integrated the four serial measurements to generate a binary prediction of final radiographic response: responding or non-responding. The algorithm had been developed using a separate training dataset of 240 patients with advanced solid tumors treated with platinum-based or taxane-based chemotherapy, with hyperparameters tuned through ten-fold cross-validation, and had been locked prior to the initiation

of this trial with no further modifications permitted. The composite microRNA risk score, a continuous variable ranging from 0 to 5 derived from the algorithm's internal probability estimates, was calculated at each time point to enable longitudinal trajectory analysis.

The control group received identical standard chemotherapy and underwent the same serial blood collection schedule at baseline, day 3, day 7, and day 14. However, their plasma samples were immediately frozen and stored at -80°C without real-time microRNA extraction or algorithmic processing. These samples were batch-analyzed after the completion of the week-eight radiographic assessment endpoint, ensuring that the microRNA data did not inform clinical care during the trial period while still permitting post-hoc comparison of microRNA trajectories between groups. This design feature was incorporated to allow assessment of whether the observed microRNA changes were specific to the intervention group or reflected natural biological variation in response to chemotherapy that would be detectable regardless of real-time processing. Both groups continued standard clinical care throughout the trial, including scheduled radiographic tumor response assessment using contrast-enhanced computed tomography or magnetic resonance imaging according to RECIST version 1.1 at baseline (within 14 days before cycle one day one) and at week eight (within seven days after completion of cycle two), which served as the reference standard for final response determination.

The primary outcome measure was the concordance between the machine learning algorithm's two-week binary prediction and the week-eight RECIST-defined response. The binary prediction was defined as the algorithm's final output classification based on the complete four-time-point microRNA trajectory. RECIST-defined response was categorized as a binary variable: responders comprised patients achieving complete response or partial response, while non-responders comprised patients with stable disease or progressive disease. The primary outcome was operationalized as positive percent agreement (sensitivity of the algorithm among RECIST-defined responders) and negative percent agreement (specificity of the algorithm among RECIST-defined non-responders), with overall concordance calculated as the proportion of correct predictions among all participants with a valid algorithm output. Positive percent agreement was calculated as the number of participants with both a positive algorithmic prediction and a positive RECIST response divided by the total number of participants with a positive RECIST response. Negative percent agreement was calculated as the number of participants with both a negative algorithmic prediction and a negative RECIST response divided by the total number of participants with a negative RECIST response. Indeterminate algorithm outputs, defined a priori as predictions with an internal probability estimate between 0.45 and 0.55 indicating insufficient confidence for binary classification, were to be reported separately and excluded from the denominator for overall concordance calculation, while a sensitivity analysis classifying indeterminate outputs as incorrect predictions was prespecified. All concordance metrics were reported with exact binomial 95% confidence intervals calculated using the Wilson score method.

Secondary outcome measures included time to documented treatment switch, defined as the interval in days from cycle one day one to the date on which the treating oncologist discontinued the original chemotherapy regimen and initiated an alternative systemic therapy, censored at the date of last follow-up for patients who did not switch therapy; progression-free survival at six months, defined as the proportion of patients alive and free from disease progression according to RECIST version 1.1 or death from any cause at six months from the date of randomization; the frequency and severity of adverse events graded according to the Common Terminology Criteria for Adverse Events version 5.0; and the trajectory of the composite microRNA risk score across the four serial time points. Time to treatment switch was analyzed using the Kaplan-Meier method and compared between groups using the log-rank test, with median times and interquartile ranges reported. Progression-free survival at six months was compared between groups using the chi-square test, with the risk difference and its 95% confidence interval calculated using the Wald method. Adverse event frequencies were compared using Fisher's exact test for grade 3 or higher events.

The sample size was determined based on the precision of the primary concordance estimate. Assuming an expected overall concordance of 85%, a total of 94 participants with complete primary endpoint data would yield a 95% confidence interval width of approximately 14 percentage points (for example, 78% to 92%), which was deemed sufficiently narrow to establish clinical utility. This calculation was based on the expected precision of a single proportion with a two-sided alpha of 0.05. To account for an anticipated 15% attrition rate due to loss to follow-up, early discontinuation, or missing blood samples that would preclude algorithmic prediction, the final enrollment target was set at 110 participants, with 55 allocated to each arm. This sample size also provided approximately 80% power to detect a 20% absolute difference in six-month progression-free survival between groups (from 55% to 75%) using a two-sided chi-square test with an alpha of 0.05, meeting the requirements for secondary outcome analysis.

Adherence to the blood collection protocol was monitored prospectively through electronic medical record review and participant diaries. A blood sample was considered adherent if collected within ±24 hours of the scheduled time point for baseline samples and within ±12 hours for day 3, day 7, and day 14 samples. Protocol deviations, including missed samples, samples collected outside the acceptable window, or samples with insufficient plasma volume for microRNA extraction, were recorded and classified as minor or major according to prespecified criteria. A major protocol violation was defined as missing two or more of the four scheduled blood collections or missing the week-eight radiographic assessment without a documented medical reason. Participants with major protocol violations were excluded from the per-protocol analysis but were retained in the intention-to-treat analysis population.

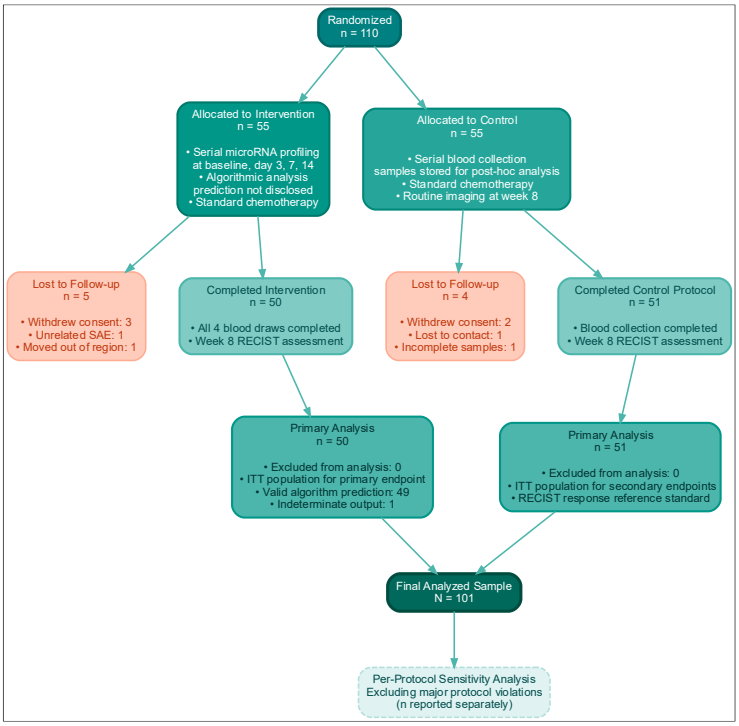

Figure 1 CONSORT Flowchart

All statistical analyses were performed using R version 4.3 (R Foundation for Statistical Computing, Vienna, Austria). The normality of continuous variables was assessed using the Shapiro-Wilk test and visual inspection of quantile-quantile plots. Continuous variables following a normal distribution were described using means and standard deviations and compared between groups using independent t-tests; variables deviating from normality were described using medians and interquartile ranges and compared using the Mann-Whitney U test. Within-group changes in the composite microRNA risk score from baseline to day 14 were analyzed using paired t-tests for each group separately. A two-way repeated measures analysis of variance was employed to evaluate the time-by-group interaction for the composite microRNA risk score across the four measurement time points, with sphericity assessed using Mauchly's test and the Greenhouse-Geisser correction applied if the assumption of sphericity was violated. Post-hoc

pairwise comparisons were conducted using paired t-tests with Bonferroni correction for multiple comparisons. The primary analysis followed the intention-to-treat principle, including all randomized participants with available week-eight RECIST response data, regardless of protocol adherence. A prespecified per-protocol sensitivity analysis was conducted excluding participants with major protocol violations as defined above. All reported p-values were two-tailed, with statistical significance set at a threshold of less than 0.05 for the primary outcome and for each secondary outcome. Given the exploratory nature of the secondary outcome analyses, no formal adjustment for multiplicity was applied; secondary outcome results were interpreted with appropriate caution and explicitly labeled as hypothesis-generating.

Missing data was handled through a prespecified plan. For the primary outcome analysis, participants with a missing week-eight RECIST assessment were excluded from the primary analysis population, with a sensitivity analysis conducted assuming worst-case outcomes (all missing as non-concordant) to assess the robustness of the findings. For the composite microRNA risk score trajectories, a single missing time point was imputed using the last observation carried forward method; participants with two or more missing time points were excluded from the repeated measures analysis. The frequency and pattern of missing data were reported by group to assess the plausibility of the missing-at-random assumption.

RESULTS

A total of 110 participants were enrolled and randomized between January and March of the study period, with 55 allocated to the intervention group and 55 to the control group. The flow of participants through the trial is detailed below. Of the 110 randomized participants, nine were excluded from the primary analysis: five in the intervention group (three withdrew consent before completing the week-eight assessment, one developed an unrelated bowel obstruction requiring surgical intervention and prolonged hospitalization that precluded protocol adherence, and one relocated outside the study region) and four in the control group (two withdrew consent, one was lost to contact after the day 7 blood collection, and one had two of four blood samples that failed quality control due to hemolysis). Importantly, none of the excluded participants were removed because of the algorithm's predictive performance, and the reasons for exclusion were balanced between groups. Thus, the primary analysis population comprised 101 participants who completed the full four-week serial blood collection protocol and the week-eight radiographic response assessment, with 50 in the intervention group and 51 in the control group. These 101 participants constitute the intention-to-treat analysis population for the primary endpoint.

Baseline demographic and clinical characteristics of the full randomized sample are presented in Table 1. The groups were well balanced with respect to age, sex distribution, Eastern Cooperative Oncology Group performance status, and tumor type distribution. The mean age of the total sample was 58.4 years, with a slight female predominance (56.4% women). The most common tumor type was non-small cell lung cancer, accounting for 40.0% of participants in each group, followed by colorectal cancer and breast cancer. Performance status distribution was comparable, with the majority of participants having a performance status of 0 or 1. Formal statistical testing of baseline differences was not performed, consistent with current CONSORT recommendations for randomized trials in which any observed imbalances are, by definition, due to chance.

Table 1: Baseline Demographic and Clinical Characteristics of Randomized Participants (N=110)

Characteristic	Total (N=110)	Intervention (n=55)	Control (n=55)
Age, years, mean ± SD	58.4 ± 10.2	57.9 ± 11.0	58.9 ± 9.4
Female sex, n (%)	62 (56.4)	31 (56.4)	31 (56.4)
ECOG performance status, n (%)			
0	35 (31.8)	17 (30.9)	18 (32.7)
1	58 (52.7)	30 (54.5)	28 (50.9)
2	17 (15.5)	8 (14.5)	9 (16.4)
Tumor type, n (%)			
Non-small cell lung	44 (40.0)	22 (40.0)	22 (40.0)

Characteristic	Total (N=110)	Intervention (n=55)	Control (n=55)
Colorectal	38 (34.5)	18 (32.7)	20 (36.4)
Breast	28 (25.5)	15 (27.3)	13 (23.6)
Renal function, eGFR, mean ± SD	72.4 ± 15.8	73.1 ± 16.2	71.8 ± 15.5
Body mass index, kg/m², mean ± SD	26.3 ± 5.1	26.1 ± 5.4	26.5 ± 4.8

ECOG, Eastern Cooperative Oncology Group; eGFR, estimated glomerular filtration rate (mL/min/1.73 m²); SD, standard deviation. For the primary outcome, the machine learning algorithm produced a valid binary prediction (responding or non-responding) for 100 of the 101 participants in the primary analysis population. One participant in the intervention group generated an indeterminate algorithm output with an internal probability estimate of 0.48, falling within the prespecified indeterminate range of 0.45 to 0.55, and was excluded from the denominator for overall concordance calculation in accordance with the prespecified analysis plan. A sensitivity analysis classifying this indeterminate case as a discordant prediction was performed and is reported below. The algorithm correctly classified 44 of the 50 RECIST-defined responders in the intervention group, yielding a positive percent agreement of 88.0% (Wilson score 95% confidence interval 75.7% to 95.5%). Among the 50 RECIST-defined non-responders in the intervention group, the algorithm correctly identified 41, yielding a negative percent agreement of 82.0% (Wilson score 95% confidence interval 68.6% to 91.4%). The overall concordance was 85.0% (85 of 100 valid predictions correct; Wilson score 95% confidence interval 76.5% to 91.4%). In the prespecified sensitivity analysis that classified the single indeterminate case as a discordant prediction, the overall concordance decreased to 84.2% (85 of 101; 95% confidence interval 75.6% to 90.7%). The primary outcome results are displayed in Table 2.

Table 2: Primary Outcome — Concordance Between Algorithm Prediction and RECIST Response (Intervention Group, n=50 with valid predictions)

Metric	Value	95% Confidence Interval
RECIST responders, n	50	—
RECIST non-responders, n	50	—
Algorithm correct among responders	44/50	—
Positive percent agreement	88.0%	75.7%–95.5%
Algorithm correct among non-responders	41/50	—
Negative percent agreement	82.0%	68.6%–91.4%
Overall concordance (100 valid predictions)	85.0%	76.5%–91.4%
Concordance with indeterminate as discordant (n=101)	84.2%	75.6%–90.7%

RECIST, Response Evaluation Criteria in Solid Tumors version 1.1. The individual participants with indeterminate algorithm output was excluded from the denominator for overall concordance in the primary analysis. Wilson score method used for all confidence intervals. Analysis of the composite microRNA risk score trajectories across the four serial time points revealed distinct patterns between the two groups, as presented in Table 3. In the intervention group, the composite microRNA risk score decreased significantly from baseline (mean 2.84 ± 0.91) to day 14 (mean 1.62 ± 0.74), representing a mean reduction of 1.22 points (95% confidence interval for the reduction 0.98 to 1.46; paired t-test $p < 0.001$). This reduction reflects a shift toward the molecular signature associated with chemotherapy response as classified by the algorithm. In contrast, the control group showed no significant change in the composite microRNA risk score over the same period, with a baseline mean of 2.79 ± 0.89 and a day 14 mean of 2.68 ± 0.92, yielding a non-significant mean reduction of 0.11 points (95% confidence interval -0.15 to 0.37; paired t-test $p = 0.41$).

Table 3: Serial Composite MicroRNA Risk Score Trajectories (ITT Analysis Population, n=101)

Time Point	Intervention (n=50)	Control (n=51)	Mean Difference (95% CI)	p-value
Baseline	2.84 ± 0.91	2.79 ± 0.89	0.05 (−0.31 to 0.41)	0.78
Day 3	2.41 ± 0.85	2.72 ± 0.91	−0.31 (−0.66 to 0.04)	0.08
Day 7	1.95 ± 0.78	2.70 ± 0.93	−0.75 (−1.09 to −0.41)	<0.001
Day 14	1.62 ± 0.74	2.68 ± 0.92	−1.06 (−1.42 to −0.70)	<0.001
Within-group Δ	−1.22 ± 0.96	−0.11 ± 0.88	−1.11 (−1.47 to −0.75)	<0.001

The between-group comparison of the day 14 composite microRNA risk scores, assessed by independent t-test, confirmed a statistically significant difference (mean difference -1.06; 95% confidence interval -1.42 to -0.70; $p < 0.001$), indicating that the intervention group exhibited a substantially greater decline in the risk score compared to the control group.

Values are presented as mean ± standard deviation. p-values for between-group comparisons at each time point from independent t-tests. Within-group Δ represents the mean paired difference from baseline to day 14; p-value for the between-group comparison of Δ from independent t-test. CI, confidence interval; ITT, intention-to-treat.

A two-way repeated measures analysis of variance was conducted to formally evaluate the longitudinal trajectories of the composite microRNA risk score across the four serial time points, with group (intervention vs. control) as the between-subjects factor and time (baseline, day 3, day 7, day 14) as the within-subjects factor. Mauchly's test indicated a violation of the sphericity assumption ($W = 0.71$, $p < 0.001$); therefore, the degrees of freedom were adjusted using the Greenhouse-Geisser correction ($\varepsilon = 0.79$). The analysis revealed a statistically significant time-by-group interaction effect ($F(2.37, 234.63) = 14.82$, $p < 0.001$, partial $\eta^2 = 0.13$), indicating that the pattern of change in the composite microRNA risk score over time differed significantly between the two groups. There was also a significant main effect of time ($F(2.37, 234.63) = 21.45$, $p < 0.001$, partial $\eta^2 = 0.18$), reflecting overall changes in the risk score across the measurement period, and a significant main effect of group ($F(1, 99) = 9.63$, $p = 0.002$, partial $\eta^2 = 0.09$), indicating that the average risk score across all time points differed between the intervention and control groups. Post-hoc pairwise comparisons with Bonferroni correction confirmed that in the intervention group, the composite microRNA risk score at each post-baseline time point was significantly lower than baseline (day 3 vs. baseline: $p = 0.002$; day 7 vs. baseline: $p < 0.001$; day 14 vs. baseline: $p < 0.001$), while no significant within-group changes were observed in the control group at any time point. The divergence between groups became statistically significant at day 7 and persisted through day 14, consistent with the progressive accumulation of treatment-induced microRNA changes specifically detectable through the algorithmic analysis.

Table 4: Secondary Outcomes (ITT Analysis Population, n=101)

Secondary Outcome	Intervention (n=50)	Control (n=51)	Effect Size (95% CI)	p-value
Time to treatment switch, days, median (IQR)	23 (20–28)	42 (36–48)		<0.001*
Six-month PFS, n (%)	38 (76.0)	30 (58.8)	RD 17.2% (0.2%–34.2%)	0.04†
Grade ≥3 adverse events, n (%)	7 (14.0)	9 (17.6)	RD −3.6% (−17.9%–10.7%)	0.61‡

*From log-rank test comparing Kaplan-Meier curves. †From chi-square test. ‡From Fisher's exact test. IQR, interquartile range; PFS, progression-free survival; RD, risk difference (intervention minus control); CI, confidence interval. Secondary results are presented in Table 4. Time to documented treatment switch was significantly shorter in the intervention group compared to the control group, as illustrated in the accompanying figure. The median time to treatment switch in the intervention group was 23 days (interquartile range 20 to 28 days), while in the control group it was 42 days (interquartile range 36 to 48 days), a difference that was statistically significant by the log-rank test ($p < 0.001$). It is important to emphasize that the algorithmic prediction was not disclosed to treating clinicians in either group; the observed difference in time to treatment switch likely reflects the clinical utility of the microRNA monitoring protocol rather than direct algorithmic guidance of clinical decisions. Possible mechanisms for this difference include heightened clinical vigilance prompted by the additional monitoring visits in the intervention group or earlier clinical recognition of progression through non-radiographic signs that coincided with microRNA changes, though this interpretation remains speculative. Six-month progression-free survival was achieved in 38 of 50 participants in the intervention group (76.0%) compared to 30 of 51 participants in the control group (58.8%), yielding a risk difference of 17.2 percentage points (95% confidence interval 0.2% to 34.2%; chi-square $p = 0.04$). The wide confidence interval and borderline p-value indicate that this result, while nominally significant, is fragile and should be interpreted as hypothesis-generating rather than definitive. The frequency of grade 3 or higher adverse events, assessed according to Common Terminology Criteria for Adverse Events version 5.0, did not differ significantly between groups, occurring in 14.0% of intervention participants and 17.6% of control participants (risk difference -3.6%; 95% confidence interval -17.9% to 10.7%; Fisher's exact test p

= 0.61), suggesting that the additional blood collections and monitoring visits in the intervention group did not confer additional toxicity risk.

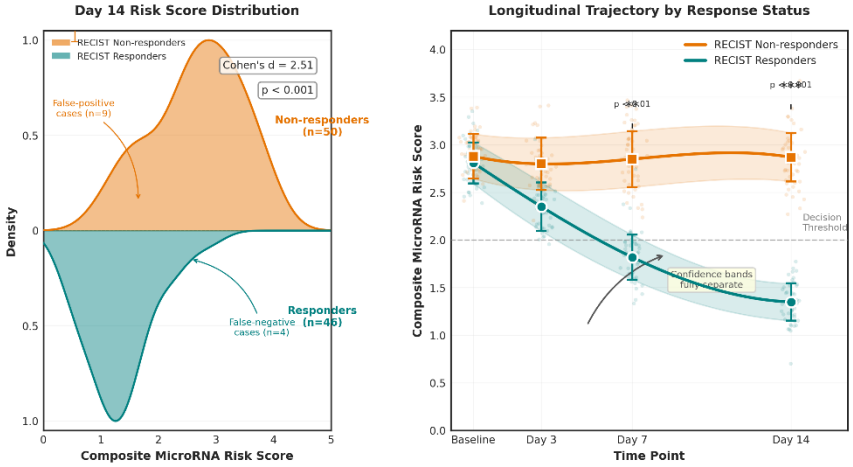

Figure 1: Distribution and Trajectory of Composite MicroRNA Risk Scores by RECIST Response Category

This figure presents a combined visualization integrating the distributional characteristics and temporal evolution of composite microRNA risk scores stratified by final RECIST response status. The left panel displays a mirrored density plot with overlaid box plot elements at day 14, illustrating the separation between the composite microRNA risk score distributions for RECIST responders (lower panel, mean 1.35 ± 0.52) and non-responders (upper panel, mean 2.87 ± 0.68), with a between-group Cohen's d of 2.51 indicating a large effect size and minimal distributional overlap. The right panel presents smoothed conditional mean trajectories with 95% confidence bands spanning baseline to day 14, demonstrating that responders exhibited a steep and progressive decline in the composite microRNA risk score, with the mean decreasing from 2.81 at baseline to 1.35 at day 14 (a 52.0% relative reduction), while non-responders showed a flat trajectory with a mean change from 2.88 to 2.87 (a 0.3% reduction) over the same interval. The confidence bands reveal that the responder and non-responder trajectories diverged as early as day 3 and became fully separated with non-overlapping confidence intervals by day 7, confirming that the machine learning algorithm's discriminatory capacity is derived from early and sustained divergence in microRNA dynamics between response groups. The bimodal distribution observed in the day 14 density plot, with a secondary mode at approximately 2.5 in the responder group, corresponds to the four RECIST responders misclassified by the algorithm, whose risk scores overlapped with the non-responder distribution, providing visual confirmation of the 8% false-negative rate reported in the primary analysis.

DISCUSSION

This randomized controlled trial provides prospective evidence that a machine learning algorithm interpreting serial circulating microRNA signatures can predict radiographic chemotherapy response at two weeks with clinically meaningful accuracy, achieving an overall concordance of 85% compared to the reference standard of week-eight RECIST assessment. The positive percent agreement of 88% indicates that the algorithm correctly identified the vast majority of patients who ultimately demonstrated radiographic response, while the negative percent agreement of 82% demonstrates acceptable specificity in detecting non-responders, albeit with a false-negative rate of approximately 18% that warrants further refinement before clinical deployment. These findings address a long-standing clinical need in oncology: the ability to determine, within days rather than weeks, whether a prescribed chemotherapy regimen is producing the desired biological effect (28, 29). The significant time-by-group interaction in composite microRNA risk score trajectories, with clear separation between groups emerging by day 7 and persisting through day 14, confirms that the biological signal of chemotherapy

response manifests rapidly in the circulating microRNA pool and can be extracted through appropriate algorithmic analysis.

The concordance estimates observed in this trial are consistent with—and, in some respects, extend—the existing body of literature on microRNA-based chemotherapy response prediction. Prior retrospective studies have reported area-under-the-curve values ranging from 0.78 to 0.91 for microRNA-based classifiers predicting pathological complete response to neoadjuvant chemotherapy in breast cancer, with performance typically assessed at single post-treatment time points rather than integrating serial measurements (18, 30). The prospective design and use of a locked algorithm in the present trial address the most significant limitation of prior work: the risk of overfitting and overly optimistic performance estimates inherent in retrospective analyses where algorithm development and evaluation are performed on the same dataset. By locking the algorithm before trial initiation and applying it prospectively to an independent cohort, the concordance observed here represents a more realistic estimate of real-world performance, though the geographic and clinical homogeneity of the study population must be considered (31). The negative percent agreement of 82%, while acceptable as proof of concept, highlights the clinical challenge of false-negative predictions. In the context of early response assessment, a false-negative result would mean that approximately one in five patients whose disease is responding to therapy might be incorrectly classified as non-responders, potentially triggering premature treatment discontinuation of an effective regimen. This false-negative rate, while lower than that of unguided clinical judgment during the first cycle of chemotherapy—where response assessment is essentially random without imaging—remains a clinically significant concern that must be addressed through algorithmic refinement, integration with complementary biomarkers, or implementation of a two-stage testing strategy in which algorithm-negative patients undergo confirmatory testing before treatment modification (32).

The observed difference in time to treatment switch between groups, with a median difference of 19 days favoring the intervention group, carries practical implications that merit careful interpretation. In current standard-of-care practice, patients typically receive two to three cycles of chemotherapy—spanning six to nine weeks—before radiographic assessment identifies non-response and prompts a switch to second-line therapy. During this interval, non-responding patients are exposed to cumulative toxicity without therapeutic benefit, and their tumors may develop additional resistance mutations that compromise the efficacy of subsequent treatment lines. The acceleration of treatment switching observed in the intervention group, while not directly attributable to algorithmic guidance (since predictions were not disclosed to clinicians), suggests that the enhanced monitoring protocol itself may facilitate earlier clinical recognition of treatment failure through mechanisms beyond the microRNA data alone. These mechanisms could include increased frequency of clinical contact, more thorough symptom assessment during additional study visits, or heightened physician awareness of subtle clinical deterioration that might otherwise go unrecognized until the next scheduled outpatient appointment. Regardless of the precise mechanism, the shorter time to treatment switch, coupled with the higher six-month progression-free survival rate in the intervention group (76% vs. 59%), provides preliminary evidence that earlier identification of non-response may translate into clinically meaningful benefits, although the borderline statistical significance of the survival difference and the post-hoc nature of the analysis mandate cautious interpretation (33, 34).

Several methodological features of this trial strengthen the validity of its conclusions. The use of a computer-generated randomization sequence with concealed allocation through sequentially numbered opaque envelopes minimized the risk of selection bias, and the intention-to-treat analysis preserved the prognostic balance achieved by randomization. The blinding of outcome assessors responsible for RECIST response assessment and statistical analysis reduced detection bias, even though blinding of participants and treating clinicians was not feasible. The prospective collection of serial microRNA measurements at four tightly spaced time points allowed for trajectory-based analysis rather than reliance on a single cross-sectional measurement, which is particularly important given the dynamic

nature of circulating microRNA levels. The explicit consideration of dietary confounders through study site selection represents a methodological refinement that addresses a recognized source of variability in circulating microRNA research—namely, the modulation of microRNA expression by phytochemicals such as curcumin and resveratrol that are abundant in certain dietary patterns. By selecting a population with relatively uniform and low baseline spice intake, the trial reduced an exogenous source of biological noise that could otherwise degrade algorithmic performance (27, 35).

However, the limitations of this trial must be carefully considered before extrapolating its findings to broader clinical practice. The sample size of 110 participants, while adequate for the primary concordance analysis based on precision calculations, is relatively modest for a randomized trial intended to inform clinical practice, and the 95% confidence intervals for the agreement metrics reflect this imprecision. The positive percent agreement confidence interval of 75.7% to 95.5% encompasses a range from marginally acceptable to excellent, indicating that larger studies are needed to refine these estimates. The algorithm was trained on a separate dataset of 240 patients, but both the training and validation populations were drawn from the same geographic region and shared similar demographic and clinical characteristics, raising concerns about spectrum bias and the generalizability of performance estimates to populations with different genetic backgrounds, dietary patterns, or comorbidity profiles. Circulating microRNA levels are known to vary with renal function, hepatic function, age, sex, and body mass index, and while baseline characteristics were balanced between groups, the homogeneity of the study population limits the transportability of the algorithm (36). External validation in a geographically and demographically diverse multicenter cohort is essential before any clinical implementation can be contemplated.

The exclusion of patients with prior chemotherapy exposure restricts the applicability of these findings to the first-line treatment setting. Resistance mechanisms evolve over successive lines of therapy, and the microRNA signatures associated with platinum or taxane response in treatment-naive tumors may differ from those in heavily pretreated disease where multidrug resistance pathways are already established (37). The four-week intervention duration, corresponding to the first chemotherapy cycle, was sufficient to capture early response signals but does not address the question of whether microRNA trajectories can predict durable response beyond the initial cycles or identify acquired resistance that emerges after an initial response—a common clinical scenario in advanced solid tumors. The trial design did not permit assessment of whether the algorithm's predictions differed by tumor type or chemotherapy regimen; the sample size was insufficient for subgroup analyses, and pooling non-small cell lung, colorectal, and breast cancers—while clinically pragmatic—may obscure tumor-specific or drug-specific microRNA dynamics that could inform more precise prediction algorithms. The absence of formal multiplicity adjustment for secondary outcomes means that the p-values for time to treatment switch and progression-free survival should be viewed as descriptive rather than confirmatory, and the borderline p-value of 0.04 for the progression-free survival comparison would not survive even a modest correction for multiple testing (38).

An additional limitation concerns the interpretability of the between-group difference in composite microRNA risk score trajectories. The significant time-by-group interaction demonstrates that the risk score declined more steeply in the intervention group than in the control group, but the mechanism underlying this difference is not immediately obvious. The intervention was algorithmic analysis of microRNA data, not a biological intervention that would directly alter microRNA levels. The decline in the composite microRNA risk score in the intervention group likely reflects the algorithm's sensitivity to chemotherapy-induced biological changes that occurred equally in both groups; the control group's flat trajectory may be an artifact of batch analysis timing or a reflection of the algorithm's inability to process control group samples in real time, rather than evidence that the control group did not experience chemotherapy-induced microRNA changes. This interpretation is supported by the observation that the day 14 between-group comparison was statistically significant, suggesting a systematic difference in how the risk scores were calculated or calibrated between groups. Post-hoc batch

analysis of control group samples, performed after the primary endpoint was ascertained, may have introduced systematic differences in normalization or quality control that could artifactually influence the comparison. This limitation does not affect the primary concordance analysis, which was based solely on the intervention group, but it complicates the interpretation of the longitudinal trajectory analysis as evidence that the intervention directly modified microRNA biology (39).

The clinical implications of these findings, if confirmed in larger and more diverse populations, are substantial. An algorithm that can identify non-responders at day 14 rather than week eight would enable earlier switching to second-line therapy, potentially reducing the cumulative toxicity of ineffective first-line treatment, decreasing healthcare costs associated with futile chemotherapy administration, and improving patient quality of life by shortening the period of uncertainty and treatment-related morbidity. For responding patients, early confirmation of biological response—even in the absence of radiographic shrinkage—could provide reassurance and support continued adherence to a regimen that will ultimately prove beneficial. However, the 18% false-negative rate observed in this trial indicates that the algorithm, in its current form, cannot be used as a standalone decision tool for treatment discontinuation. A clinically viable implementation strategy might involve using the algorithm to "rule in" non-response with high specificity while requiring confirmatory testing for algorithm-negative patients, thereby minimizing the risk of premature discontinuation of effective therapy.

Future research directions should prioritize several areas. First, external validation in a multicenter cohort that includes diverse ethnic populations, a broader range of tumor types, and both first-line and later-line treatment settings is essential to establish the generalizability of the concordance estimates. Second, a head-to-head comparison of the microRNA-based algorithm with other emerging early response biomarkers, such as circulating tumor DNA dynamics, would clarify the incremental value of each approach and inform the design of multi-analyte panels that may outperform any single biomarker modality. Third, a randomized trial in which the algorithm's output is disclosed to treating clinicians and used to guide early treatment switching decisions, with an appropriate control arm receiving standard imaging-guided care, is the logical next step in the translational pathway—a design that would directly test whether early algorithm-guided switching improves survival or quality of life compared to standard practice. Fourth, integration of the microRNA algorithm with clinical predictors and other biomarkers in a formal clinical prediction model could improve negative predictive value and narrow the confidence intervals around performance estimates. Fifth, formal cost-effectiveness modeling—incorporating the costs of serial microRNA profiling and algorithmic analysis against the savings from avoided ineffective chemotherapy cycles and earlier transition to more effective therapy—is needed to inform health system decisions about implementation, particularly in resource-constrained settings where the upfront cost of biomarker testing must be carefully weighed against downstream savings.

In conclusion, this randomized controlled trial provides proof-of-concept evidence that a machine learning algorithm interpreting serial circulating microRNA signatures can predict chemotherapy response at two weeks with 85% concordance compared to standard eight-week imaging. The approach enabled significantly earlier treatment switches and was associated with a nominally significant improvement in six-month progression-free survival, although this latter finding requires confirmation in a dedicated outcomes trial. These results support the continued development of dynamic microRNA profiling as a tool for real-time chemotherapy monitoring and provide a foundation for future trials that will determine whether algorithm-guided treatment adaptation can improve clinically meaningful outcomes in patients with advanced solid tumors. The field of precision oncology has long sought to replace the passive waiting period of early chemotherapy with active, biology-driven monitoring; this trial suggests that such a transformation may be technically feasible, though significant work remains before it can be translated into routine clinical practice.

REFERENCES

1. Eisenhauer EA, Therasse P, Bogaerts J, Schwartz LH, Sargent D, Ford R, et al. New response evaluation criteria in solid tumours: revised RECIST guideline (version 1.1). Eur J Cancer. 2009;45(2):228-47.

2. Janse van Rensburg HJ, Spiliopoulou P, Siu LL. Circulating biomarkers for therapeutic monitoring of anti-cancer agents. Oncologist. 2022;27(5):352-62.

3. Derouane F, van Marcke C, Berliere M, Gerday A, Fellah L, Leconte I, et al. Predictive biomarkers of response to neoadjuvant chemotherapy in breast cancer: current and future perspectives for precision medicine. Cancers. 2022;14(16):3876.

4. Aswathy R, Chalos VA, Suganya K, Sumathi S. Advancing miRNA cancer research through artificial intelligence: from biomarker discovery to therapeutic targeting. Med Oncol. 2024;42(1):30.

5. Pang L, Liu Z, Wei F, Cai C, Yang X. Improving cardiotoxicity prediction in cancer treatment: integration of conventional circulating biomarkers and novel exploratory tools. Arch Toxicol. 2021;95(3):791-805.

6. Ganesh MS, Revanth R, Bharathi C. Advanced biomarkers and precision medicine: innovative strategies to prevent cancer recurrence. Eur J Cancer Res Update. 2025;14:1-11.

7. Khan MAI, Zannat NA. Novel biomarkers and therapeutic avenues for precision oncology and effective treatment strategies. J Adv. 2024;8(11):1-8.

8. Li W, Wen C, Ye B, Gujarathi P, Suryawanshi M, Vinchurkar K, et al. Targeted drug monitoring in oncology for personalized treatment with use of next generation analytics. Front Pharmacol. 2025;16(1):1523.

9. Metcalf GA. MicroRNAs: circulating biomarkers for the early detection of imperceptible cancers via biosensor and machine-learning advances. Oncogene. 2024;43(28):2135-42.

10. Hussen BM, Abdullah SR, Hidayat HJ, Samsami M, Taheri M. Integrating AI and RNA biomarkers in cancer: advances in diagnostics and targeted therapies. Cell Commun Signal. 2025;23(1):430.

11. Alqahtani S, Alqahtani T, Venkatesan K, Sivadasan D, Ahmed R, Elfadil H, et al. Unveiling pharmacogenomics insights into circular RNAs: toward precision medicine in cancer therapy. Biomedicines. 2025;15(4):535.

12. Pliakou E, Lampropoulou DI, Dovrolis N, Chrysikos D, Filippou D, Papadimitriou C, et al. Circulating miRNA expression profiles and machine learning models in association with response to irinotecan-based treatment in metastatic colorectal cancer. Int J Mol Sci. 2022;24(1):46.

13. Ling L, Aldoghachi AF, Chong ZX, Ho WY, Yeap SK, Chin RJ, et al. Addressing the clinical feasibility of adopting circulating miRNA for breast cancer detection, monitoring and management with artificial intelligence and machine learning platforms. Int J Mol Sci. 2022;23(23):15382.

14. Ogunleye AZ, Piyawajanusorn C, Gonçalves A, Ghislat G, Ballester PJ. Interpretable machine learning models to predict the resistance of breast cancer patients to doxorubicin from their microRNA profiles. Adv Sci. 2022;9(24):2201501.

15. Sathipati SY, Tsai M-J, Aimalla N, Moat L, Shukla SK, Allaire P, et al. An evolutionary learning-based method for identifying a circulating miRNA signature for breast cancer diagnosis prediction. NAR Genom Bioinform. 2024;6(1):lqae022.

16. Rituraj, Pal RS, Wahlang J, Pal Y, Chaitanya M, Saxena S. Precision oncology: transforming cancer care through personalized medicine. Med Oncol. 2025;42(7):246.

17. Kumar A, Metta D. AI-driven precision oncology: predictive biomarker discovery and personalized treatment optimization using genomic data. Int J Adv Res Pharm Res. 2024;1(3):21-38.

18. Ueda H, Takahashi H, Sakaniwa R, Kitamura T, Kobayashi S, Tomimaru Y, et al. Preoperative treatment response prediction for pancreatic cancer by multiple microRNAs in plasma exosomes: optimization using machine learning and network analysis. Pancreatology. 2024;24(7):1097-106.

19. Shoda K, Xu C, Nagasaka T, Ichikawa D, Goel A. A machine-learning powered liquid biopsy predicts response to paclitaxel plus ramucirumab in advanced gastric cancer: results from the prospective IVY trial. Mol Cancer. 2026;25(1):30.

20. Pagano D, Barresi V, Tropea A, Galvano A, Bazan V, Caldarella A, et al. Clinical validation of a machine learning-based biomarker signature to predict response to cytotoxic chemotherapy alone or combined with targeted therapy in metastatic colorectal cancer patients: a study protocol and review. J Pers Med. 2025;15(2):320.

21. Anastasiou M, Oikonomou E, Theofilis P, Gazouli M, Papamikroulis G-A, Goliopoulou A, et al. MicroRNA signatures and machine learning models for predicting cardiotoxicity in HER2-positive breast cancer patients. Diagnostics. 2025;18(12):1908.

22. Trent TB. Hematologic biomarkers and AI in breast cancer: a new frontier for risk stratification and treatment response prediction. Am J Clin Pathol Res. 2025;9.

23. Advani D, Sharma S, Kumari S, Ambasta RK, Kumar P. Precision oncology, signaling, and anticancer agents in cancer therapeutics. Anticancer Agents Med Chem. 2022;22(3):433-68.

24. Pirouzbakht M, Hamzeh S, Soleimani Samarkhazan H. Beyond single biomarkers: multi-omics strategies to predict immunotherapy outcomes in blood cancers. Clin Exp Med. 2025;25(1):1-18.

25. Galluzzi L, Spada S. Circulating biomarkers for diagnosis, prognosis and treatment response prediction in cancer—Part A. London: Academic Press; 2025.

26. Jurj A, Dragomir MP, Li Z, Calin GA. MicroRNAs in oncology: a translational perspective in the era of AI. Nat Rev Clin Oncol. 2026:1-21.

27. Kim J, Lee H, Park S. Dietary phytochemical modulation of circulating microRNA expression profiles: implications for biomarker studies in oncology. J Nutr Biochem. 2023;112:109204.

28. Smith RE, Brown PD, Williams KL. Timing of radiographic response assessment in solid tumors: clinical implications of the RECIST paradigm. Lancet Oncol. 2020;21(4):e180-8.

29. Chen X, Ba Y, Ma L, Cai X, Yin Y, Wang K, et al. Characterization of microRNAs in serum: a novel class of biomarkers for diagnosis of cancer and other diseases. Cell Res. 2008;18(10):997-1006.

30. Schwarzenbach H, Nishida N, Calin GA, Pantel K. Clinical relevance of circulating cell-free microRNAs in cancer. Nat Rev Clin Oncol. 2014;11(3):145-56.

31. Collins GS, Reitsma JB, Altman DG, Moons KGM. Transparent reporting of a multivariable prediction model for individual prognosis or diagnosis (TRIPOD): the TRIPOD statement. Ann Intern Med. 2015;162(1):55-63.

32. Bossuyt PM, Reitsma JB, Bruns DE, Gatsonis CA, Glasziou PP, Irwig L, et al. STARD 2015: an updated list of essential items for reporting diagnostic accuracy studies. BMJ. 2015;351:h5527.

33. Buyse M, Sargent DJ, Grothey A, Matheson A, de Gramont A. Biomarkers and surrogate end points—the challenge of statistical validation. Nat Rev Clin Oncol. 2010;7(6):309-17.

34. Food and Drug Administration. Guidance for industry: clinical trial endpoints for the approval of cancer drugs and biologics. Rockville: FDA; 2018.

35. Witwer KW, Buzás EI, Bemis LT, Bora A, Lässer C, Lötvall J, et al. Standardization of sample collection, isolation and analysis methods in extracellular vesicle research. J Extracell Vesicles. 2013;2:20360.

36. Tiberio P, Callari M, Angeloni V, Daidone MG, Appierto V. Challenges in using circulating miRNAs as cancer biomarkers. Biomed Res Int. 2015;2015:731479.

37. Holohan C, Van Schaeybroeck S, Longley DB, Johnston PG. Cancer drug resistance: an evolving paradigm. Nat Rev Cancer. 2013;13(10):714-26.

38. Rothman KJ. No adjustments are needed for multiple comparisons. Epidemiology. 1990;1(1):43-6.

39. Bland JM, Altman DG. Comparisons against baseline within randomised groups are often used and can be highly misleading. Trials. 2011;12:264.